Ice Accretion on Wind Turbine Blades

Hudecz, Adriána; Koss, Holger; Hansen, Martin Otto Laver

Published in:
Proceedings of the 15th International Workshop on Atmospheric Icing of Structures (IWAIS XV)

Publication date:
2013

Ice Accretion on Wind Turbine Blades

Adriána Hudecz[#1], Holger Koss [*2], Martin O. L. Hansen [#†3]

[#]*Department of Wind Energy, Technical University of Denmark*
[1] ahud@dtu.dk
[3] molh@dtu.dk

[*]*Department of Civil Engineering, Technical University of Denmark*
[2] hko@byg.dtu.dk

[†]*Centre for Ships and Ocean Structures, Department of Marine Technology, Norwegian University of Science and Technology*

***Abstract* — In this paper, both experimental and numerical simulations of the effects of ice accretion on a NACA 64-618 airfoil section with 7° angle of attack are presented. The wind tunnel tests were conducted in a closed-circuit climatic wind tunnel at Force Technology in Denmark. The changes of aerodynamic forces were monitored as ice was building up on the airfoil for glaze, rime and mixed ice. In the first part of the numerical analysis, the resulted ice profiles of the wind tunnel tests were compared to profiles estimated by using the 2D ice accretion code TURBICE. In the second part, Ansys Fluent was used to estimate the aerodynamic coefficients of the iced profiles. It was found that both reduction of lift coefficient and increase of drag coefficient is a nearly linear process. Mixed ice formation causes the largest flow disturbance and thus the most lift degradation. Whereas, the suction side of the rime iced ice profile follows the streamlines quite well, disturbing the flow the least. The TURBICE analysis agrees fairly with the profiles produced during the wind tunnel testing.**

I. Introduction

In cold climate areas with temperatures below 0°C and humid environment for larger periods of the year icing represents an significant threat to the performance and durability of wind turbines (Tammelin et al. [1], Tallhaug et al. [2] and Baring-Gould et al. [3]). In this paper, both experimental and numerical simulations of the effects of ice accretion on a NACA 64-618 airfoil section are presented. The experiments were performed in a closed-circuit climatic wind tunnel at FORCE Technology in Denmark. Aerodynamic forces were monitored throughout the icing process for 7° angle of attack at different temperatures, which were used to ensure adequate environment for the typical ice types, rime, glaze and mixed ice, which threaten the operation of wind turbine.

There were already a number of wind tunnel tests conducted on iced airfoils in the past. Seifert and Richert [4] and Jasinski et al. [5] used artificial ice deposits during their experiments. In case of Seifert and Richert's tests [4], the molds were made of actual ice fragments from a wind turbine, whereas Jasinski et al. [5] simulated the ice profiles with Nasa's ice accretion code, LEWICE. Hochart et al. [6] performed two-phase experiments. In the first phase, the ice deposit was grown and then in the second phase, efficiency tests were performed. The main difference from these tests and the ones presented in this paper is the fact that the aerodynamic forces were monitored as ice was accumulating. At the end of the tests, the ice profiles were documented by contour tracing for further, numerical analysis.

In the recent years, especially due to the increased computer power, it became possible to determine the performance of iced wind turbine much faster and more accurately with computational fluid dynamics (CFD) and panel method based models. Homola et al. [7] have used a two-steps method, combining TURBICE and Ansys Fluent to investigate the effect of ice similarly on a NACA 64-618 profile. TURBICE is comprehensive numerical ice accretion software from VTT, Technical Research Centre of Finland, which uses panel method to calculate the potential flow. It was verified by icing wind tunnel testing of both aircraft and wind turbine airfoils. The accuracy of the solution is dependent on the number of the panels and their distribution around the section (Makkonen et al., [8]). Homola et al. [7] found that the lift coefficient was reduced in all cases and the smallest change was observed in case of rime ice. During the CFD simulations, it was found that the horn type glaze ice shape causes the largest separation, which leads to a significantly reduced lift and higher drag coefficient.

Etemaddar et al. [9] has also used the same profile in their numerical analysis. In their study, they combined Nasa's LEWICE code with Ansys Fluent and pointed out that the ice load increases with liquid water content (LWC), median volumetric diameter (MVD) and relative wind speed.

The numerical simulations presented in this paper were carried out in two parts. First, the collected ice profiles were compared to profiles generated in TURBICE. In the second part, numerical analyses were done on the iced profiles from the wind tunnel tests in Ansys Fluent.

The aim of the wind tunnel tests was to investigate the changes of aerodynamics as ice built up on the airfoil for glaze, rime and mixed ice tests. The relative changes of lift and drag coefficients along with the shape of the ice deposits could be compared to results of the numerical analysis.

II. Abbreviations and Nomenclature

AOA, α – angle of attack
C_L – lift coefficient
C_D – drag coefficient
D – drag force
G_{ice} – gravity force of ice deposit
L – lift force
LWC – liquid water content
MVD – median volumetric diameter
SP – separation point
U – mean wind speed

III. Methods

In this section, both experimental and numerical set-up of the analyses is detailed.

A. Wind Tunnel Tests – Experimental Setup

The tests were performed in the Collaborative Climatic Wind Tunnel (CWT) at FORCE Technology. The wind tunnel was developed and built as a collaboration project between Technical University of Denmark and FORCE Technology. The main specifications are listed in TABLE I.

TABLE I Basic specifications of the wind tunnel (based on Georgakis et al. [10])

Temperature	-5 to 40 °C
Minimum liquid water content (LWC)	0.2 g/m^3
Test section cross-sectional area	2.0x2.0 m
Test section length	5 m
Maximum wind speed velocity	31 m/s
Turbulence intensity	0.6 to 20 %

NACA 64-618 airfoil section (900 mm chord length and 1350 mm width) provided by LM Wind Power was used during the experiments. A pair of AMTI MC5 force and torque transducers was used to measure the loading simultaneously around 6 degrees of freedom. Based on the measured forces (F_x and F_y), which are visualized in Fig. 1, and the known angle of attack (α) and wind speed (U), the lift (L) and drag (D) forces along with the weight of ice (G_{ice}) can be calculated.

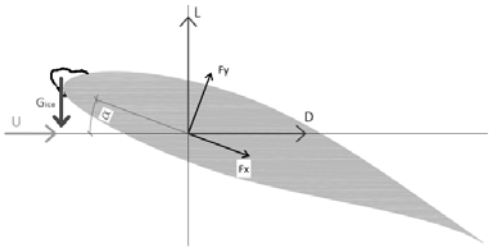

Fig. 1. Forces acting on the iced airfoil. F_y and F_x are directly measured by the force transducers and based on these and the known angle of attack and wind speed (U), the lift (L) and drag (D) forces along with the weight of ice (G_{ice}) can be calculated.

The tests were performed by first setting the target wind speed and temperature in the test section. A constant angle of attack, 7° was used in these experiments. As soon as the target temperature was reached, the water spray, and thus in-cloud environment, was set. For glaze and mixed ice tests, 15 m/s wind speed was applied during ice build-up while for the rime ice test due to the limitation of the wind tunnel's cooling unit, it was necessary to reduce the wind speed to 10 m/s in order to ensure cold enough temperature. The ice accretion process was running for 60 minutes and every five minutes the forces were measured. Based on the force measurements, not only the aerodynamic forces but also the gravity force of the accumulated ice was calculated. In order to study the pure effect of the altered airfoil profile, this force was subtracted from the lift measurements. At the end of the tests, the ice profiles were documented by contour tracing and were used in the numerical simulation part.

The flow in a wind tunnel is different from that, which occurs in the free-air due to the presence of the tunnel walls, therefore the measurements were corrected by following ESDU 76028, *Lift-interference and blockage corrections for two-dimensional subsonic flow in ventilated and closed wind-tunnels methodology* [11].

The specifications of the presented tests are summarized in TABLE II. The temperatures listed here are the mean values of the established temperature during the tests. The MVD and LWC values are target values based on the specification of the manufacturer of the spray nozzles (Schick [12]).

TABLE II The specification of the presented tests.

	Glaze ice test	Mixed ice test	Rime ice test
AOA (°)	7	7	7
T (°C)	-3	-5	-8
MVD (μm)	25	25	20
LWC (g/m^3)	0.7	0.7	0.7
U_{accr} (m/s)	15	15	10
U_{test} (m/s)	15	15	15

B. Numerical Simulation Setup – TURBICE.

TURBICE simulations were performed at VTT, Technical Research Centre of Finland in order to compare the results of the wind tunnel tests to a numerical ice accretion model. For the air temperature only a constant value can be defined in the simulation program. Hence, mixed ice simulation could not be modeled. There are a number of other input parameters, such as MVD, LWC, meteorological wind speed, rotating speed of the wind turbine, pitch angle, air temperature, air pressure and accretion time. These parameters were set to ensure similar conditions as it was in the wind tunnel.

Since the MVD and LWC were only target values in the wind tunnel tests, several scenarios were analyzed in TURBICE and only the best fits are presented here. The input parameters of the different tests are listed in TABLE III.

TABLE III Input Parameters for the presented Turbice Tests

Parameters	Glaze test 1.	Glaze test 2.	Rime test 1.	Rime test 2.
AOA (°)	7	7	7	7
MVD (μm)	25	30	25	25
LWC (g/m^3)	0.65	0.65	0.4	0.6
Temp (°C)	-3	-3	-8	-8
Time (min)	60	90	60	90

C. *Numerical Simulation Setup – Ansys Fluent.*

CFD simulations are used to analyze numerically the impacts of ice accretion on the flow behavior and on the aerodynamic characteristics of the airfoil. As it was mentioned before, the ice profiles were collected at the end of the wind tunnel tests and were further analyzed by Ansys Fluent. Since the ice profiles were collected from specific locations, 2D models were done. The construction and meshing of each model was done using Ansys Workbench. The control volume around the blade was rectangular with edges positioned at 50 chords length away in vertical direction and 20 chords length from the horizontal direction (cross flow). It was necessary to set the horizontal boundaries further away to avoid any effect caused by these boundaries on the flow around the airfoil.

An inflation layer was added to the mesh in order to produce a structured, fine mesh in the vicinity of the airfoil to achieve a better representation of the flow near the airfoil surface. The first layer height is dependent on the surface roughness, since the roughness height may not exceed it. However, it was found that Ansys Fluent cannot properly handle surface roughness; therefore it was not included in the analysis. In TABLE IV, the setup of the inflation layer is listed. The height of the first layer was set small enough to ensure the validity of the log law.

TABLE IV SETUP OF INFLATION IN ANSYS MODEL

	Clean profile	Glaze ice test	Mixed ice test	Rime ice test
First layer height (m)	1e-5	1e-5	1e-5	1e-5
Nr. of layers of inflation layer	40	40	40	35
Growth rate	1.2	1.2	1.2	1.2

In Fig. 2, an example of the mesh around the leading edge is shown. An appropriate size was chosen for the quadrilaterals so they can follow the complex curve of the ice deposit.

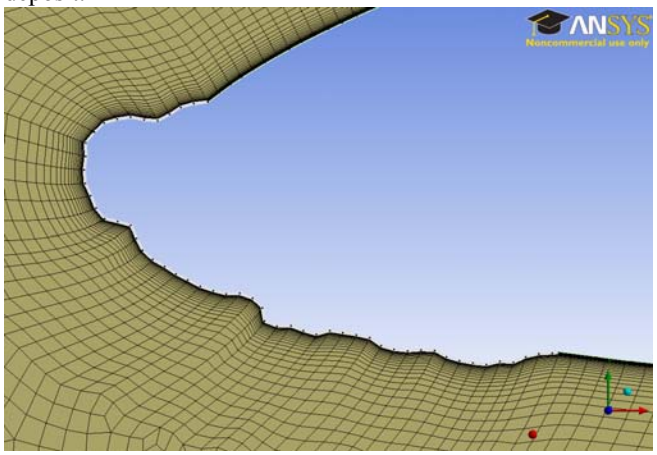

Fig. 2 Mesh around the iced leading edge in case of glaze iced airfoil. The height of the first layer is 1e-5 m and there are 40 layers in the inflation layer.

During the simulation Spalart-Allmaras and k-Ω SST turbulence models were used. It was found in previous studies (e.g. Mortensen [13]) that the solution using Spalart-Allmaras model converges faster and easier than with the k-Ω SST turbulence model. Therefore the first 500 iterations were done by using Spalart-Allmaras model providing an initial guess for the k- Ω SST turbulence model and achieving more stable convergence. However, Chung and Addy [14] pointed out that Spalart-Allmaras model is the best performing model when simulating ice accretions; therefore that model was used for the iced profiles.

IV. RESULTS

The above discussed simulations' results are presented in this section. It should be kept in mind that these values are only valid for the set-up used in these particular tests.

A. *Wind tunnel tests*

The forces caused by the wind acting on the iced airfoil along with the gravity force of ice were measured throughout the accretion process. Based on these force measurements, it was possible to calculate the lift and drag coefficient of the continuously altered airfoil. The reduction of the lift coefficient as a function of accretion time for the three different ice types is shown in Fig. 3. As it is seen, first order polynomials could be fitted to the points, thus the degradation process is almost linear. Even though the accretion time was only 60 minutes, significant changes were monitored. The lift coefficient decreased the least, 22 % in case of rime ice tests and most significant for mixed ice tests, 34 %. For the glaze ice test, the degradation was 25 %.

The degradation is already visible after 5 minutes into the accretion. This sudden drop seems to be more severe than the one happened between 5 and 10 min. The slope of the drop in the first 5 minutes is much steeper than of the polynomials fitted to the points.

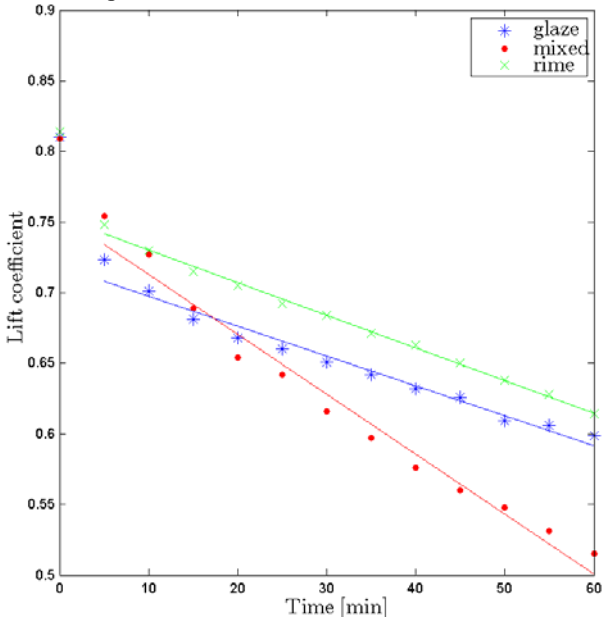

Fig. 3 Alteration of lift coefficient as a function of ice accretion time for 7° AOA in case of glaze (*), mixed (.) and rime ice (x). The environmental

conditions were the following: LWC~0.7 g/m^3, MVD~25 for glaze and mixed ice and MVD~20 for rime ice and Re~1e6.

An increase of drag force and hence an increase of drag coefficient was experienced during the tests. This tendency is illustrated in Fig. 4. Similarly to the initial lift coefficient degradation, rapid increase of drag coefficient can be observed in the first five minutes. However, contrary to the lift curves, the process does not seem to slow down, i.e. the slope of the initial increase does not differ significantly from the slope of the fitted polynomials. It is clearly visible in Fig. 4 that the smallest increase of the drag coefficient occurs under rime ice conditions.

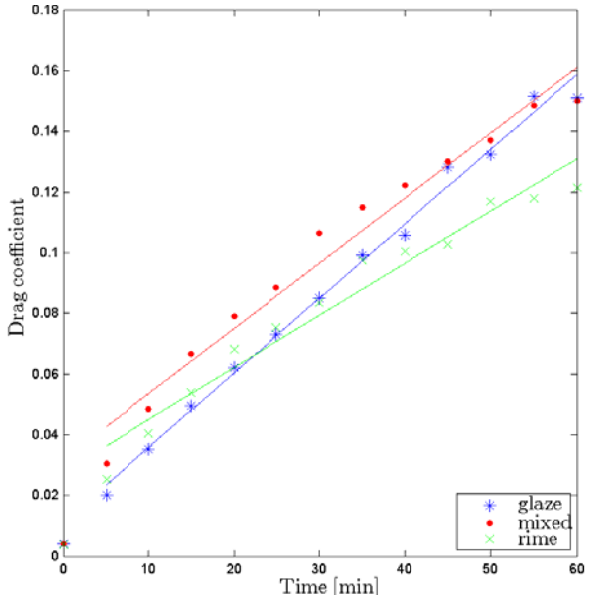

Fig. 4 Alteration of drag coefficient as a function of ice accretion time for 7° AOA in case of glaze (*), mixed (.) and rime ice (x). The environmental conditions were the following: LWC~0.7 g/m^3, MVD~25 µm for glaze and mixed ice and MVD~20 for rime ice and Re~1e6.

In Fig. 5, the collected ice profiles are shown. It can be seen, that the smallest ice deposit was building up in case of the rime ice test while the largest one in case of the mixed ice test. The rime ice accreted only on the leading edge of the airfoil, whereas the other two types accumulated also on the pressure side of the airfoil. The stagnation point is quite clear in all three cases (marked with orange circles in Fig. 5).

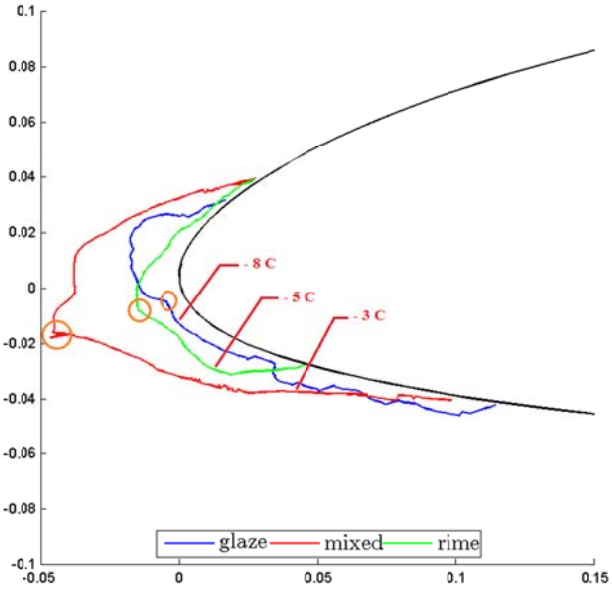

Fig. 5 Collected ice profiles from the wind tunnel tests for α=7° after 60 minutes of accretion. The environmental conditions were the following: U~15 m/s, LWC~0.7 g/m^3, MVD~25 for glaze and mixed ice and U~10m/s, MVD~20 for rime ice. The orange circles illustrates the stagnation points.

B. Numerical Simulation – TURBICE

As it was mentioned above, it was only possible to simulate conditions resulting in glaze and rime ice accretion on the airfoil. The results are plotted against the shapes collected from the climatic wind tunnel tests. Fig. 6 shows the results from the glaze simulations. The red curve represents the profile collected from the wind tunnel for LWC~0.7 g/m^3, MVD~25 µm, the blue line illustrates the result from TURBICE with LWC~0.65 g/m^3, MVD~25 µm during 60 minutes of accretion time, whereas the TURBICE results of LWC~0.65 g/m^3, MVD~30 µm and 90 minutes of accretion time are plotted in green.

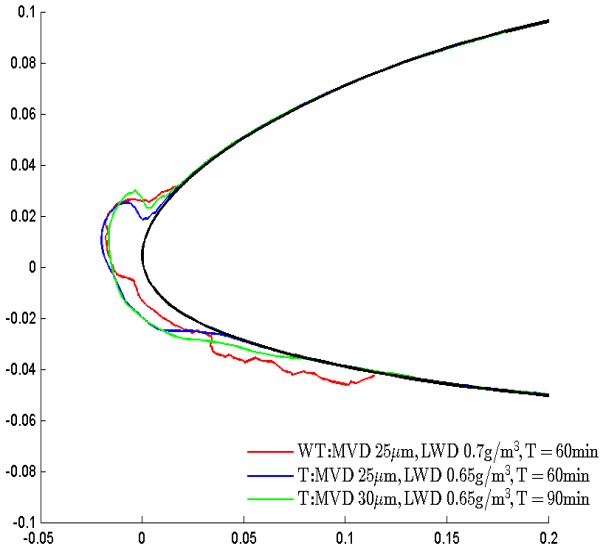

Fig. 6 Ice profiles from both the wind tunnel (WT) test and TURBICE (T) simulations for glaze ice. The red curve represents the profile collected from the wind tunnel for LWC~0.7 g/m^3, MVD~25 µm, the blue line illustrates the result of LWC~0.65 g/m^3, MVD~25 µm during 60 minutes of accretion time, whereas the results of LWC~0.65 g/m^3, MVD~30 µm and 90 minutes of accretion time plotted in green.

In Fig. 7, the results of the rime ice test are shown. The red curve represents the profile collected from the wind tunnel for LWC~0.7 g/m^3, MVD~20 µm, the blue line illustrates the result from TURBICE of LWC~0.4 g/m^3, MVD~25 µm during 60 minutes of accretion time, whereas the results of LWC~0.6 g/m^3, MVD~25 µm and 90 minutes of accretion time from TURBICE are plotted in green.

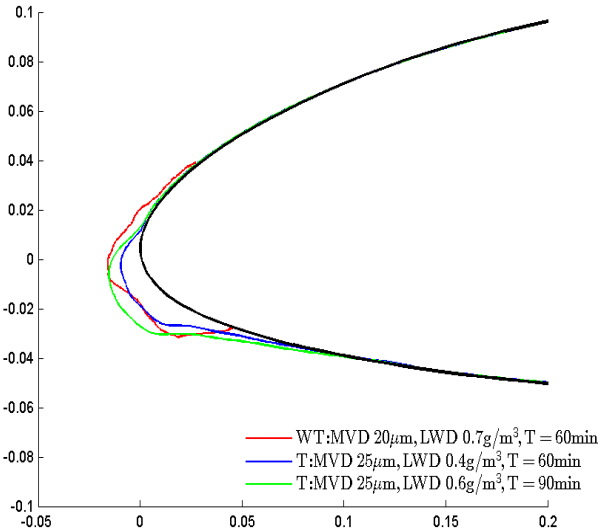

Fig. 7 Ice profiles from both the wind tunnel (WT) test and TURBICE (T) simulations for rime ice. The red curve represents the profile collected from the wind tunnel for LWC~0.7 g/m^3, MVD~20 µm, the blue line illustrates the result of LWC~0.4 g/m^3, MVD~25 µm during 60 minutes of accretion time, whereas the results of LWC~0.6 g/m^3, MVD~25 µm and 90 minutes of accretion time plotted in green.

C. Numerical Simulation – Ansys Fluent

The results of the numerical simulation with Ansys Fluent are summarized in TABLE V. The relative change refers to the reduction of lift coefficient of iced airfoil related to the lift coefficient of the clean profile. As it can be read from the table, mixed ice accretion caused the most significant reduction of lift coefficient whereas the least was found for rime ice.

TABLE V RESULTS OF NUMERICAL SIMULATIONS BY ANSYS FLUENT

Test	C_L	Relative change [%]
Clean profile	1.01	-
Glaze iced profile	0.784	22
Mixed iced profile	0.762	25
Rime iced profile	0.831	18

In Fig. 8, the velocity vectors colored by the velocity magnitude around the leading edge of the clean airfoil are shown. The color-range represents the flow speed around the airfoil ranging from 0 to 22m/s (blue to red). It can be seen that the incoming velocity decreases to 0 m/s at the stagnation point (represented by blue arrows) and speeds up at the suction side. The flow around the airfoil is rather smooth and well attached.

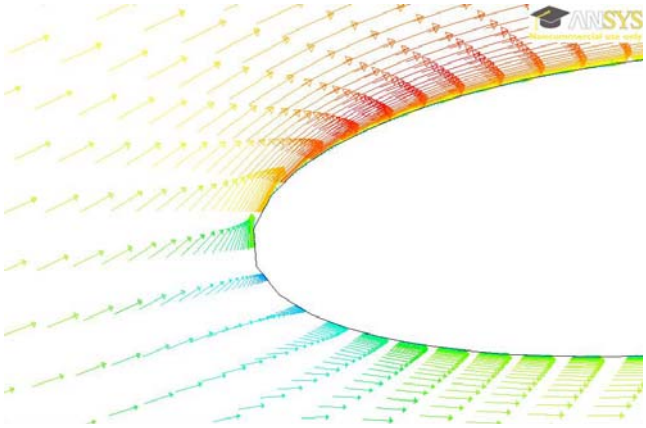

Fig. 8 Velocity vectors colored by the velocity magnitude (m/s) around the clean airfoil for inlet velocity 14 m/s and α=7°. The color-range from 0 to 22 m/s.

In Fig. 9, Fig. 10 and Fig. 11 the velocity vectors colored by the velocity magnitude around the leading edge of the iced airfoil is shown for glaze, mixed and rime ice, respectively. It can be seen that the ice deposit in each case disturbs the flow quite significantly. SP1 and SP2 illustrated the flow separation points at the suction and pressure side, respectively.

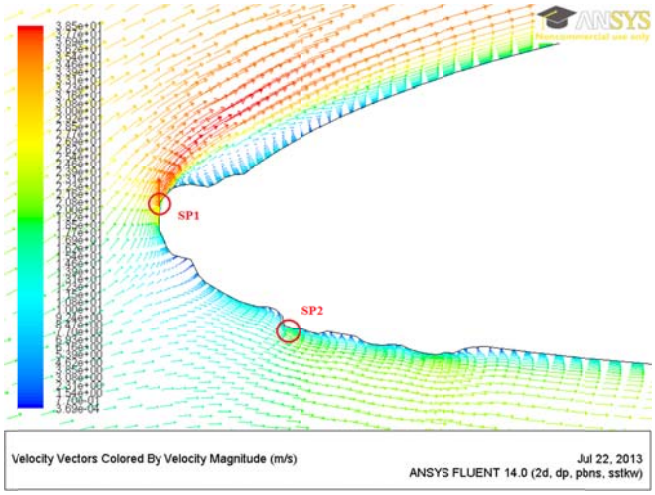

Fig. 9 Velocity vectors colored by the velocity magnitude (m/s) around the glaze iced airfoil for inlet velocity 14 m/s and α=7°. The color-range from 0 to 22 m/s. SP1 and SP2 illustrated the flow separation points at the suction and pressure side, respectively.

A large separation bubble is formed behind the leading edge separation point 1 (SL1) on the suction side of the airfoil, see Fig. 9.

In case of mixed ice deposit, a peak (SP1) was formed around the stagnation point, which reduces the flow speed at the suction side (see Fig. 10). A "nose" shaped ice formation can be also seen around the stagnation point, which was not seen in case of the other two types of ice simulations.

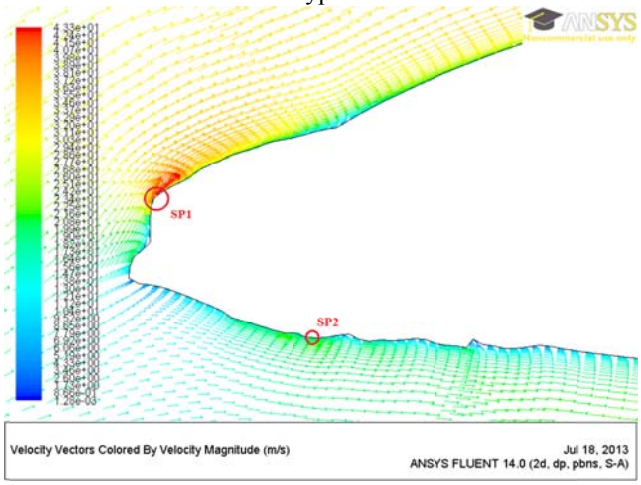

Fig. 10 Velocity vectors colored by the velocity magnitude (m/s) around the mixed iced airfoil for inlet velocity 14 m/s. The color-range from 0 to 22 m/s. SP1 and SP2 illustrated the flow separation points at the suction and pressure side, respectively.

At the suction side in Fig. 11, the accreted rime ice caused small disturbance on the flow pattern, compared to the clean airfoil. However, multiple local separation points can be found on the suction side (marked with red circles), which are causing lower slightly lower velocity zones compared to the clean profile.

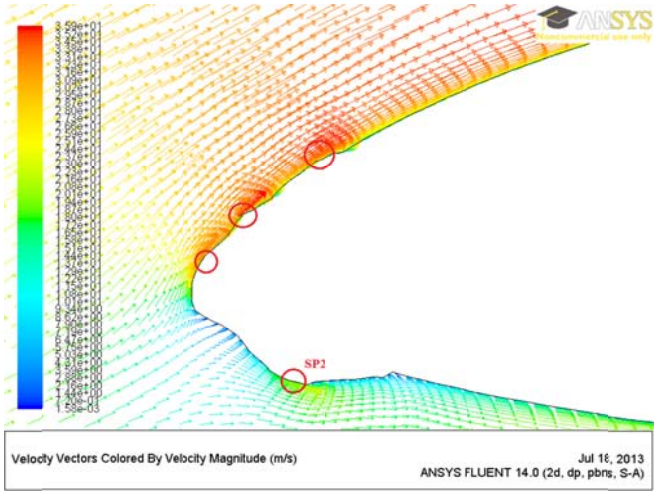

Fig. 11 Velocity vectors colored by the velocity magnitude (m/s) around the rime iced airfoil for inlet velocity 14 m/s and α=7°. The color-range from 0 to 22 m/s. SP2 illustrated the flow separation points at the pressure side, whereas there are multiple separation points marked by red circles at the suction side.

At the pressure side, small recirculation zones can be spotted behind the ice peaks (SL2) for each ice tests.

V. Discussion

A. *Wind Tunnel Tests*

The results of the wind tunnel tests shows that the lift coefficient decreased whereas the drag coefficient increased for all three ice types (see Fig. 3 and Fig. 4). The same conclusion was drawn in the studies mentioned in the *Introduction*. However, Jasinski et al. [5] showed that in some cases of rime ice accretion, the lift coefficient increased. This behavior was not experienced during the tests presented in this paper.

It can be observed from Fig. 3 that the initial degradation in the first 5 minutes is highly significant in each test, and hence if the reduction would follow this trend, the lift degradation would be much more severe. The immediate reduction of lift coefficient was caused by the changed surface roughness, as it was also shown by e.g. Lynch and Khodadoust [15].

It can be also noticed in Fig. 3, that the difference between the immediate reduction of lift coefficient for the different ice types is not significant, which indicates that the initial degradation is independent of the ice formation type for the same angle of attack.

It was also found that the least lift decrease and drag increase were caused by rime ice accretion. It is because in case of rime ice, the water droplets freeze on impact at the leading edge and this deposit acts as an extended leading edge causing less flow disturbance. For glaze and mixed ice, some of the droplets did not freeze on the surface but ran off along the airfoil and freeze aft, which resulted in larger iced surface area (see Fig. 5), and thus more disturbed flow field. The mixed ice profile had the highest negative influence on the flow and therefore it caused the highest lift degradation.

B. Numerical Simulation – TURBICE

Fig. 6 and Fig. 7 shows the results of TURBICE analyses for both rime and glaze ice together with the wind tunnel results for comparison. The TURBICE profiles and the profiles from the wind tunnel tests were not identical; however, they were in good agreement considering the circumstance that LWC and MVD are not known in the wind tunnel experiment. This leads to that these parameters could not be set accurately for the TURBICE simulation. Since it was not possible to measure LWC and MVD accurately in the wind tunnel, it was not possible to set the correct values in TURBICE. This could be a reason for the differences.

Some of the TURBICE tests used 90 minutes accretion time, which is longer than the duration of the wind tunnel tests. However, this should not be a major issue, because it was seen that the ice build-up is a nearly linear process. Therefore it can be assumed that the shape of an ice profile accreted in 60 minutes is similar to the one presented here.

C. Numerical Simulation – Ansys Fluent.

The trend of the reduction of lift coefficients agrees quite well with the wind tunnel test results. However, the relative degradation was found to be lower than it was for the experiments. The reason could be that with the contour tracing method, the small changes of surface roughness could not be documented therefore they were not implemented in the numerical analysis.

It was seen that the glaze and mixed ice formations caused the most flow disturbance. The sharp edges at the suction side seen in both Fig. 9 and Fig. 10 led to a speed up, which caused a large separation bubble especially in case of glaze ice. In case of rime iced profile, the flow followed a similar pattern as it was observed for the clean airfoil and comparing Fig. 11 and Fig. 8, the magnitude of the velocity did not differ significantly from the clean profile. For all three cases, there were some vortex formations noticed behind the ice peaks at the pressure side causing recirculation zones, which lead to some flow disturbance and retardation. However, it seems that they do not have a large influence on the change of the overall leading edge aerodynamics.

VI. CONCLUSION

Both experimental and numerical analyses have been performed to study the effect of glaze, rime and mixed ice accretion on the aerodynamics of an iced NACA 64-618 profile for 7^{o} angle of attack. The experiments were carried out in a climatic wind tunnel, and for the numerical analyses, TURBICE ice accretion model and Ansys Fluent were used to verify the findings from the wind tunnel tests.

During the wind tunnel tests, the aerodynamic forces were monitored as ice was building up on the surface. Similarly to other studies and also to the numerical investigation, lift coefficient was found to decrease and drag coefficient increased as ice accreted. These processes were found to be nearly linear.

Mixed ice formation caused the most severe lift coefficient reduction, whereas the least was found for rime ice. The largest ice deposit accreted on the profile in case of mixed ice and thus the largest disturbance was seen here. The flow around the rime iced ice profile followed a pattern similar to the streamlines around the clean profile, hence causing low disturbance.

The ice accretion model TURBICE was used to estimate ice profiles for similar conditions as it was set in the wind tunnel. These profiles agree, considering the limitations of known experimental boundary conditions, fairly with the profiles produced during the wind tunnel testing.

It can be concluded that significant lift reduction and thus power production loss can be achieved even in the first hour of ice accretion.

ACKNOWLEDGMENT

Force Technology, LM Wind Power and Cowifonden are acknowledged for allowing us to use their unique facility to conduct the tests, for lending the NACA 64-618 profile and for the financial support, respectively. The authors would also like to acknowledge VTT, Technical Research Centre of Finland, for the support they provided for using TURBICE ice accretion model.

REFERENCES

[1] B. Tammelin, M. Cavaliere, H. Holttinen, C. Morgan, H. Seifert, and K. Santti, Wind energy production in cold climate (WECO). Technical report, Finnish Meteorological Institute, 1998.

[2] L. Tallhaug, G. Ronsten, R. Horbaty, R. Cattin, T. Laakso, M. Durstewitz, A. Lacroix, E. Peltola, and T. Wallnius, "Wind energy projects in cold climate. Technical report, Executive Committee of the International Energy Agency Programme for Research and Development on Wind Energy Conversion Systems, 2009.

[3] I. Baring-Gould, R. Cattin, M. Durstewitz, M. Hulkkonen, A. Krenn, T. Laakso, A. Lacroix, E. Peltola, G. Ronsten, L. Tallhaug, and T. Wallenius. 13. Wind Energy Projects in Cold Climates. Technical report, 2011.

[4] H. Seifert and F. Richert. Aerodynamics of iced airfoils and their influence on loads and power production. European Wind Energy Conference, 1997.

[5] W. J. Jasinski, S. C. Noe, M. S. Selig, and M. B. Bragg. Wind turbine performance under icing conditions. Journal of Solar Energy Engineering, ASME, 120(1):60-65, 1997.

[6] C. Hochart, G. Fortin, and J. Perron. Wind turbine performance under icing conditions. Wind Energy, 11:319333, 2008.

[7] M. C. Homola, M. S. Virk, T. Wallenius, P. J. Nicklasson, and P. a. Sundsbø. Effect of atmospheric temperature and droplet size variation on ice accretion of wind turbine blades. Journal of Wind Engineering and Industrial Aerodynamics, 98(12):724–729, 2010.

[8] L. Makkonen, T. Laakso, M. Marjaniemi, and K. J. Finstad. Modelling and prevention of ice accretion on wind turbines. Wind Energy, 25(1):3–21, 2001.

[9] M. Etemaddar, M. O. L. Hansen and T. Moan. Wind turbine aerodynamic response under atmospheric icing conditions. Wind Energy, DOI: 10.1002/we.1573, 2012.

[10] C. Georgakis, H. Koss, and F. Ricciardelli. Design specifications for a novel climatic wind tunnel for the testing of structural cables. International Symposium on Cable Dynamics (ISCD) - 8, 2009, Paris, France.

[11] ESDU 76028, Lift-Interference and Blockage Corrections for Two-Dimensional Subsonic Flow in Ventilated and Closed Wind Tunnel, ESDU 1976.

[12] R. J. Schick. Spray technology reference guide: Understanding drop size, bulletin 459c. Technical report, Spraying Systems Co.
[13] K. Mortensen, CFD Simulation of an airfoil with leading edge ice accretion, Department of Mechanical Engineering, Technical University of Denmark, 2008
[14] J.J. Chung and H.E. Addy, Jr. A Numerical Evaluation of Icing effects on a Natural Laminar Flow Airfoil. NASA TM-2000-209775, January 2000.
[15] F. T. Lynch and A. Khodadoust. Effects of ice accretions on aircraft aerodynamics. Progress in Aerospace Sciences, 37(8):669-767, 2001.